In: AIAA SciTech Forum 2023, 23-27 January 2023, National Harbor, Maryland, USA
DOI:10.2514/6.2023-0670

AI-Based Multifidelity Surrogate Models to Develop Next Generation Modular UCAVs

Hasan Karali *, Gokhan Inalhan † and Antonios Tsourdos ‡
Cranfield University, MK43 0AL, United Kingdom

The next generation low-cost modular unmanned combat aerial vehicles (UCAVs) provide the opportunity to implement innovative solutions to complex tasks, while also bringing new challenges in design, production, and certification subjects. Solving these problems with tools that provide fast modeling in line with the digital twin concept is possible. In this work, we develop an artificial intelligence (AI) based multifidelity surrogate model to determine performance parameters of innovative modular UCAVs. First, we develop a data generation algorithm that includes a high-fidelity model based on computational fluid dynamics methods and a low-fidelity model based on computational aerodynamic approaches. In the next step, a new transfer learning-based surrogate model is generated using multifidelity data. Thanks to this approach, the developed AI model more accurately predicted the flow conditions that were missing in the high-fidelity data with the data obtained from the low-order model. The performance of the proposed AI-based surrogate model is to be investigated in terms of accuracy, robustness, and computational cost using a generic modular UCAV configuration.

I. Introduction

FUTURE battlespace is expected to be dominated by unmanned combat systems with major advances in autonomy. In the first stage, these systems are planned to fulfill the tasks given both in formation and separately under the tactical command of a manned leadership in the Manned-Unmanned Teaming (MUM-T) concept [1]. According to this theme, the Unmanned Combat Aerial Vehicles (UCAVs) will potentially have intelligence gathering, electronic warfare, air-to-air and air-to-ground combat capabilities via their artificial intelligence-enabled autonomy [2]. In addition, it is considered that these systems can be used not only with fighter jets but also with other types of aircrafts such as tankers, bombers, and transports in different scenarios [3].

Low prices are the most prominent feature of these "Attritable/Reusable" or "Loyal/Robotic wingman" concept UCAVs. In the U.S. Air Force terminology attritable/reusable term is used to define a new class of UAVs that low cost, which means cheaply enough to be lost in combat and then affordably replaced, highly reliable, and have a few years of the life cycle [4]. To be more specific, according to the mission equipment they carry, while the unit cost of these vehicles is expected to be between $2-15 million, the unit cost of an operational latest F-16 variant is between $64-80 million and the F-35 is around $100 million [5, 6]. When life cycle cost (LCC) is taken into account, this difference will increase in favor of low-cost UCAVs [7, 8]. In addition, it is possible to field several low-cost attritable UCAVs for $10.9 million, which is the pilot combat ready training cost of the F-22, a manned 5th-generation air superiority aircraft [9]. Because the cost directly affects the mass, a future air force can consist of much greater number of UCAVs than jet fighters [10]. Considering their ability to perform independent missions, they can be deployed and stored in many different locations. All this will enable such systems to deploy, produce and sustain mission sorties at a sufficient pace to generate and preserve combat mass in a contentious battlefield [11]. As can be seen from Fig. 1, many companies are interested in such concepts.

The UCAVs in the flexible mission concept carry various equipment according to the different operational tasks. This equipment can be expressed as changing sensors, radar systems, and payloads. Besides, performance requirements such as endurance, range, maneuverability, and radar cross-section area also vary according to the task. As a consequence of the multi-role concept, adaptable modular configurations become inevitable. The adaptable configuration mentioned here includes a "plug and play (PNP)" design philosophy for both the hardware/software and the main aircraft components such as wings, fuselage sections, and engines. As a case in point, MQ-28A , developed by the Boeing Airpower Teaming System, is expected to carry various unnamed sensors on its reconfigurable nose to conduct particular Intelligence

*PhD Student, School of Aerospace, Transport and Manufacturing, hasan.karali@cranfield.ac.uk, AIAA Member
†BAE Systems Chair, Professor of Autonomous Systems and Artificial Intelligence, inalhan@cranfield.ac.uk, AIAA Associate Fellow
‡Professor, School of Aerospace, Transport and Manufacturing, a.tsourdos@cranfield.ac.uk

Surveillance, Reconnaissance (ISR) scenarios [12]. Similarly, in Royal Air Force's The Lightweight Affordable Novel Combat Aircraft (LANCA) project, a rapidly reconfigurable UAV is pointed out to perform different roles, including intelligence, surveillance, and reconnaissance (ISR), electronic warfare, and strike missions [13]. On the Kratos XQ-58, in addition to the modular nose and payload section, the wing and wing leading edges are planning to exchange to meet changing mission requirements [4].

(a) Boeing MQ-28 [14]

(b) Kratos XQ-58 [15]

(c) EADS Barracuda [16]

(d) HAL CATS Warrior [17]

(e) Spirit AeroSystems Mosquito [18]

(f) General Atomics Gambit [19]

Fig. 1 Attritable/Reusable UCAV concepts

The open architecture of a proposed modular UCAV, which is suitable for continuous updating, necessitates an innovative approach in both design, production, and certification processes. The modular system, which contains a large number of combinations, will generate many configurations and at the end of the design process, each of them must go through a different certification procedure. Here, serious and effort-demanding problems arise such as the connection of different structural parts, their strength in different operational conditions, and the ability of connected sets to meet flight performance requirements. A possible solution to the problem at hand is digital engineering (DE). This approach could provide significant long-term development, production, operations, and sustainment efficiencies in these type game-changing programs [20]. For example, General Atomics' Autonomous Collaborative Platform (ACP), known as Gambit, is designed using digital engineering to accelerate its market time and reduce acquisition cost [19]. Especially digital twins provide great benefits in design optimization and upgrade analysis, performance validation and optimization, product improvement and calibration [21]. As seen in the development process of Boeing T-7, an advanced jet trainer program, the precise digital twins of each aircraft are generated for upgrades, enhancements, and data-driven maintenance, both for the real product and its digital copy throughout their life cycle. Thus, the company provides a 25% reduction in development time, a 50% reduction in software costs, and an 80% reduction in assembly hours or 200 fewer people to design and build [22].

Taken from a broad perspective, it is possible to optimize the design of UCAV for each specific scenario. In a modular design, changeable lifting surfaces (wing, tail, or canard), nose, and payload section, propulsion systems can be generated, and these components can be brought together in a lego-like structure. As illustrated in Fig. 2 , the proposed concept includes several modular components. For instance, a wing with a smaller span and reduced radar cross-section area can be used in the combat mission , while large wings that allow for carrying higher weights for longer times could be used for the ISR mission. Determining the most suitable components for each mission scenario ends up with searching for different optimum points in an extensive design space. The optimization procedure needs huge calculations and iterations to reach the optimum point, such as using traditional methods to obtain relevant aerodynamic, structural-like features is difficult due to time and computational costs. To overcome this issue, numerical evaluation can be applied through a surrogate model that calculates the performance characteristics of given configurations. In this study, AI-based multifidelity surrogate analysis tools will be developed to both design optimization and digital twin models of complete modular UCAVs.

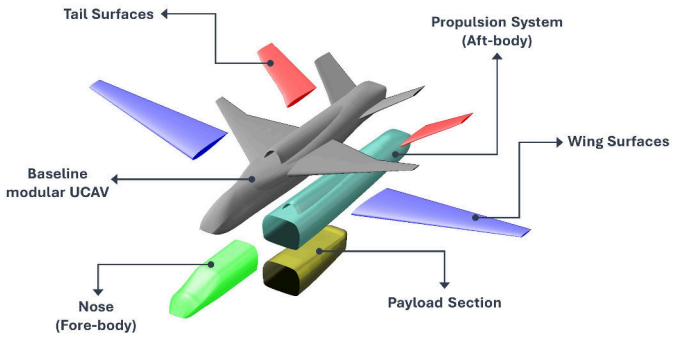

Fig. 2 Proposed modular UCAV configuration

As is known, different performance, life cycle cost, and stealth requirements result in different designs and flight regimes. However, when the up-to-date UCAVs are examined, a concentration in the high-subsonic/transonic regime is observed as seen in Fig. 3. Transonic flow regime means that there are both subsonic and supersonic airflow around the vehicle. There will be dramatic increases in drag and separations in flow due to shock waves that occur while in this regime. At this point, considering the complexity of the flow, computationally expensive computational fluid dynamics (CFD) based analysis tools are generally preferred. However, in the early phases of design studies, thousands of aerodynamic analyses are required for the combination of different geometries and flow conditions as a part of design optimization. For this reason, it is preferable to use low-order methods, which are much cheaper computationally than CFD methods, but also provide lower accuracy [23]. To overcome this problem surrogate models are used in several applications.

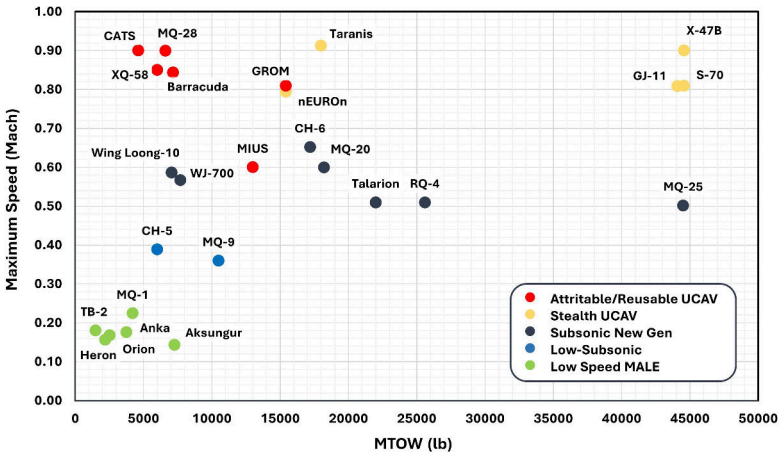

***Some data are obtained from official/unofficial sources as an estimated or targeted performance parameter**

Fig. 3 Maximum speed vs maximum take-off weight of combat UAVs

When the literature is examined, it is observed that surrogate model algorithms are frequently used in two-dimensional turbine blade or airfoil optimization [24] [25–37]. In addition, there are surrogate models used in transonic and supersonic wing optimization. Several statistical or machine learning-based surrogate model studies can be found in the literature [38–44]. When artificial intelligence-based surrogate models are compared with classical methods, it has been observed that as the data set grows, classical methods with statistical approaches become unnecessary and there is the order of magnitude differences in favour of AI methods in terms of computation time [45]. However, there are question marks about the robustness of AI-based models. For this reason, there is a gap in the literature regarding a comprehensive AI-based surrogate model with mixed fidelity. Also in our previous studies, we have developed a deep learning based surrogate model [46] using data generated by our low-fidelity NLLT aerodynamic tool [47] which can characterize the nonlinear aerodynamic performance of conventional small UAVs. In these studies, we have experienced that AI-based surrogate models are fast and accurate tools with very strong interpolation capability, and we further developed the reduced order model and used it as an aero solver in an optimization application [48]. With the surrogate

aerodynamic model developed in this study, we show that both the flight performance parameters and the aerodynamic loads on the configuration can be calculated quickly and accurately. Specifically, in this paper, we aim to illustrate that the trustworthy surrogate model from the mix-fidelity data set can be used as a solver in the design optimization cycle.

In the context of this study, we focused on the transfer learning approach, unlike previous studies, to predict the aerodynamic performance of configurations. The difference between transfer learning from traditional machine learning algorithms is that learning a new task is based on previously learned tasks. The main idea behind transfer learning is to extract knowledge from some related domains to help a neural network algorithm to achieve better performance in the domain of interest [49, 50]. In general, current progress in transfer learning is on the use of image-based convolutional neural networks for classification or clustering problems. However, in this study, we will apply Network-Based Deep Transfer Learning capabilities for multifidelity regression problems. Network-based deep transfer learning can be explained as the reusing of the partial network that is pre-trained in the source domain, including its network structure and connection parameters, and transfer it to be a part of a deep neural network used in the target domain [51]. The need for transfer learning occurs when there is a limited supply of target training data. This may be because the data is rare, the data being expensive to collect and label, or the data being inaccessible [52]. Therefore, transfer learning is an approach that can solve the problem of aerodynamic analysis methods in the design cycle described previously.

The rest of the paper is organized as follows: In the “Methodology” section, the main algorithm of the paper is briefly given. In the "Multifidelity Aerodynamic Performance Modelling" section, aerodynamic models are explained, providing insight into their mathematical basis. In the “Surrogate Performance Modelling via Machine Learning” section, in-depth information is given about data sets, sampling algorithm, and the structure of the machine learning algorithm. In the "Application of the Model" section, an example application of the developed model is performed. Finally, the conclusions are presented, and the objectives planned to be achieved in future studies are explained.

II. Methodology

The performance of an aircraft is mainly related to geometry, flow direction, Reynolds number and Mach number. For the main performance parameters, lift (C_L) and drag coefficients (C_D), this relationship can be expressed as follows:

$$C_{L,D} = f(Geometry, \alpha, \mathrm{Re}, M) \tag{1}$$

in here Reynolds number is about boundary layer development while the Mach number is about compressibility. In order to determine these parameters, solution methods are used in which the flow is modeled and complex equation sets are tried to be solved. However, with a capable regression model and sufficient data, it is possible to eliminate this whole process. A performance mapping between given function inputs and aerodynamic performance coefficient outputs is possible with machine learning algorithms.

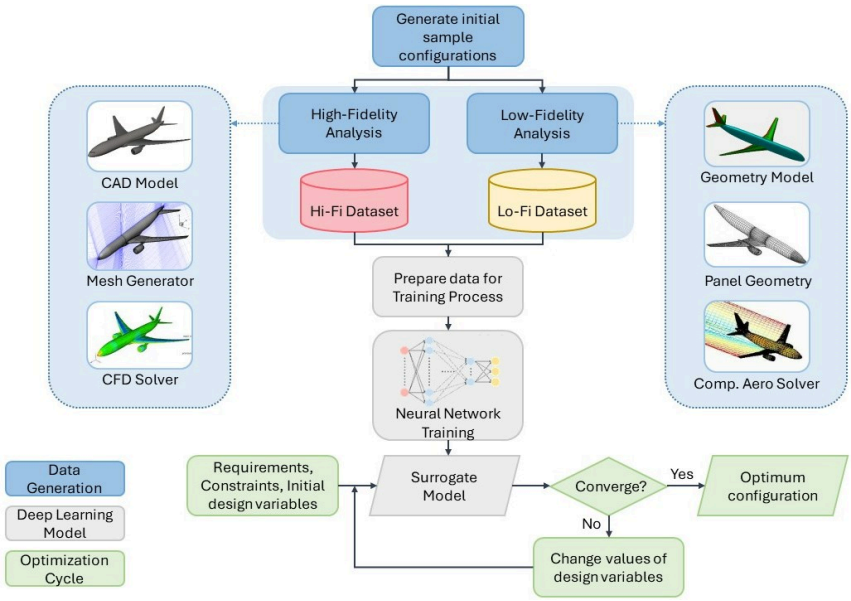

Fig. 4 Surrogate model-based design optimization algorithm

Our proposed approach is illustrated in Fig. 4. In this proposed approach, firstly, configurations are generated in the design space by using sampling algorithms. In the next step, a high-fidelity dataset based on SU2 [53] CFD tool and a low-fidelity dataset based on VSPAERO [54] are generated. After that artificial neural network-based multifidelity surrogate model is developed as the main focus of the study. Transfer learning has been integrated into this model, making it more generalizable, reliable, and robust.

Additionally, we tested the algorithm using the generic modular UCAV configurations. The generic combat UAV configuration given in Fig. 5 is used in both data generation and test applications. This configuration simply consists of a wing, fuselage, and a V-tail. More detailed information about this model can be found in the data generation section below.

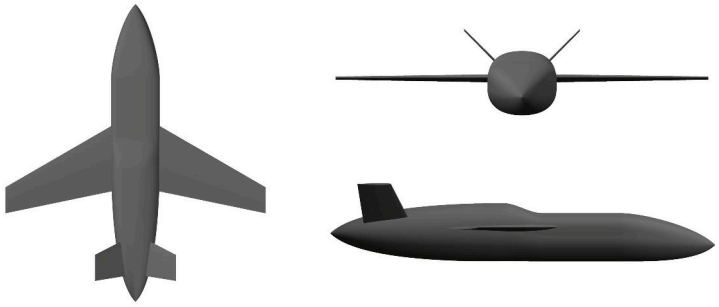

Fig. 5 Baseline UCAV configuration

III. Multifidelity Aerodynamic Performance Modelling

As the basis of the geometry model, the open-source Vehicle Sketch Pad (OpenVSP) software of NASA is used, which allows the user to create three-dimensional parametric models of generic aircraft configurations defined by common engineering parameters [55]. OpenVSP's ability to quickly generate configurations and export this geometry in different formats provides usability in the conceptual and preliminary design processes [56, 57]. In this study, OpenVSP - Python API integration was preferred, which provides coding flexibility to design a large number of configurations.

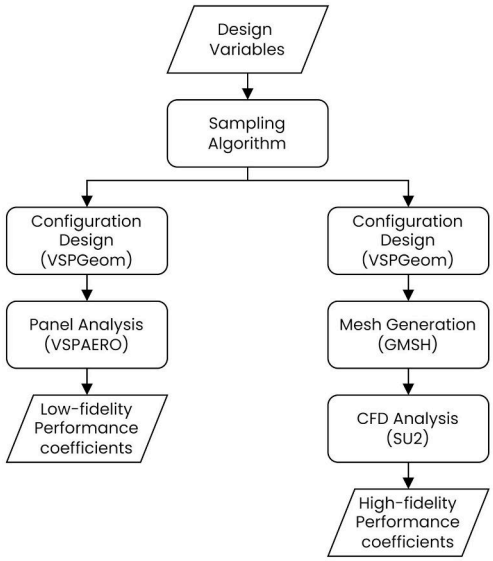

Fig. 6 Multifidelity aerodynamic performance modelling algorithm

The generic UCAV configurations were analyzed with the VSPAERO panel method as a low-fidelity analysis tool and with SU2 CFD solver as high fidelity tool. The mesh required for CFD analysis was generated using OpenVSP and

GMSH [58]. All these integrations are provided through the Python script prepared for the project. A representative flow diagram of the algorithm is given in Fig. 6.

The aerodynamic models and their mathematical backgrounds are briefly explained in the following subsections. In addition, in subsection C, the performance of these models was validated by comparing them with an experimental study.

A. Low Fidelity Aerodynamic Model

Low-order aerodynamic models are used to predict aircraft performance cheaply and quickly by making some assumptions in flow conditions and geometry. Although the potential flow-based panel methods, which is one of the well-known computational aerodynamics methods, provide more complex geometry modeling and solution than semi-empirical, lifting line and vortex lattice methods (VLM), it remains at a lower level compared to CFD solutions. Because this approach uses the simplest form obtained from the Navier-Stokes equations describing the flow, neglecting all viscous and heat transfer terms. When the impact of these assumptions is considered physically, it becomes clear that skin friction drag, separation, and transonic shocks cannot be calculated [59]. However, panel methods also have advantages over other computational aerodynamic methods such as the vortex lattice method. While VLM models ignore thickness and apply boundary conditions (BCs) on an average mean surface, panel methods can model blunt geometries and apply BCs on the actual surface.

Panel methods can be briefly described as numerical schemes used to solve the linear, inviscid, irrotational flow equation at subsonic or supersonic freestream Mach numbers. The name of the equation that panel codes solve is the Prandtl-Giauert equation. For steady subsonic flow this equation is usually can be defined as:

$$\tilde{\nabla}^2\phi = \left(1 - M_\infty^2\right)\phi_{xx} + \phi_{yy} + \phi_{zz} = 0 \tag{2}$$

For subsonic flows, Eq. (2) is elliptical. This type of equation allows any disturbance to be felt everywhere in the flow field, although the effect usually disappears with distance. To model the effect of the geometry on the flow, the singularities are distributed over the entire geometry and their strengths are calculated over the surface velocity boundary conditions. The velocities induced by each ring vortex at a specified control point are calculated using the law of Biot-Savart. The contribution of each vortex loops and trailing wakes at a given i control point is calculated as follows:

$$\vec{V}_i = \sum_j^{\text{Loops}} \left[\vec{V}_{\text{loop}}\right]_j + \sum_j^{\text{Wakes}} \left[\vec{V}_{\text{wake}}\right]_j \tag{3}$$

Then freestream velocity component is added to the induced velocity and tangency boundary condition applied as:

$$\left[\vec{V}_\infty + \vec{V}_i\right] \cdot \hat{n}_i = 0 \tag{4}$$

In the panel method model, shade wakes are represented as vortex filaments that leave the sharp trailing edges of wings and possibly bodies. The strength of these filaments is determined by the Kutta condition, which allows the flow to leave the trailing edge properly. Also in VSPAERO, the location of these vortex filaments is solved iteratively in the overall flow field solution. Further details of the panel method algorithm can be found in the literature [60]. At the end of the process, the whole problem is reduced to the solution of a set of linear equations:

$$A\vec{x} = \vec{b} \tag{5}$$

where $\vec{x}$ represents the unknown circulation strengths. To reduce the computational cost, VSPAERO use an iterative method, the generalized minimal residual method (GMRES), for the numerical solution of this system of linear equations.

$$\vec{R}_i = \vec{b} - A\vec{x}_i \tag{6}$$

where $\vec{R}_i \rightarrow \overrightarrow{0}$ as $i \rightarrow \infty$. Using preconditioned GMRES algorithm, matrix-free evaluation of the residual is obtained. In this application, Precondition matrix was selected as an approximate LU decomposition of A. After calculating the strength of the singularities, the aerodynamic forces and moments affecting the geometry are obtained.

Various correction factors are used to take into account the local compressible effects that occur especially in the high-speed subsonic regime. The most popular of these is the Prandtl-Glauert rule, but a better model, the Karma-Tsien rule, is used in this study. In this model, the freestream Mach number is used to correct the pressure coefficient (C_p). It is defined as:

$$C_p = \frac{C_{p0}}{\sqrt{1 - M_\infty^2} + \left[M_\infty^2 / \left(1 + \sqrt{1 - M_\infty^2} \right) \right] C_{p0}/2} \tag{7}$$

where M_∞ is the freestream Mach number and C_{p0} is the potential flow coefficient of pressure. Since the panel method gives an inviscid solution, the parasite drag values are calculated with a semi-empirical approach.

Table 1 VSPAERO general analysis parameters

Parameters	Values
Mach Correction	Karman-Tsien Rule
Stall Model	Carlson Pressure Distribution
Preconditioner	Matrix
Number of Wake Iteration	5
Number of Wake Nodes	64

VSPAero general analysis parameters are summarized in Table 1. The wake iteration is limited to 5 as it can be seen in the analysis settings. Because, usually sufficient convergence rate is achieved in the third iteration.

B. High Fidelity Aerodynamic Model

High-order aerodynamic models are used to predict aircraft performance with high accuracy. In this study, a compressible Euler solver is selected as a high fidelity model. In this model, the viscous and thermal conductivity terms are neglected from the Navier-Stokes equation and the compressible Euler equations are obtained. These equations can be defined in differential form as [61]:

$$\mathcal{R}(U) = \frac{\partial U}{\partial t} + \nabla \cdot \bar{F}^c(U) - S = 0 \tag{8}$$

where S is a generic source term, the conservative variables are the working variables and are given by

$$U = \{\rho, \rho\bar{v}, \rho E\}^\top \tag{9}$$

where ρ is the fluid density, E is the total energy per unit mass, p is the static pressure, and the convective flux is

$$\bar{F}^c = \begin{Bmatrix} \rho\bar{v} \\ \rho\bar{v} \otimes \bar{v} + \bar{\bar{I}}p \\ \rho E\bar{v} + p\bar{v} \end{Bmatrix} \tag{10}$$

In the Euler solver, the equations are discretized in space using a finite volume method on a vertex-based schemes. As a solution inviscid performance coefficients are obtained. In the algorithm, the skin friction drag calculated by the OpenVSP module is added to the SU2 solution and the total drag value is calculated.

C. Validation of Aerodynamic Models

In this subsection, the accuracy of existing aerodynamic models will be tested using NASA's wind tunnel experimental study. The experiment was carried out in the Langley high-speed 7- by 10-foot tunnel using a closed test section. The test geometry, consisting of a swept wing and fuselage suitable for the UCAV configuration, was tested at high subsonic flow and various aerodynamic force-moment parameters were collected. In addition, jet boundary and blockage corrections were applied to the static aerodynamic results. Table 2 summarizes parameters related to testing geometry and flow conditions.

Table 2 Wind tunnel model geometry and flow parameters

Parameters	Values
Fuselage Length	123.95cm
Fuselage Diameter	12.45cm
Airfoil	NACA 63A408
Wing Area	0.139m2
Span	91.4cm
Root Chord	21.8cm
Tip Chord	8.71cm
Sweep	35°
Mach	0.5
Dynamic Pressure	≈ 310lb/ft2

The results obtained from the analysis are illustrated together with the experimental data in Fig. 7. It is clearly observed that the panel method results are close to the experimental data, especially in low angles of attack. In this study, the panel method provided an acceptable level of accuracy, since the analysis was performed under cruise conditions.

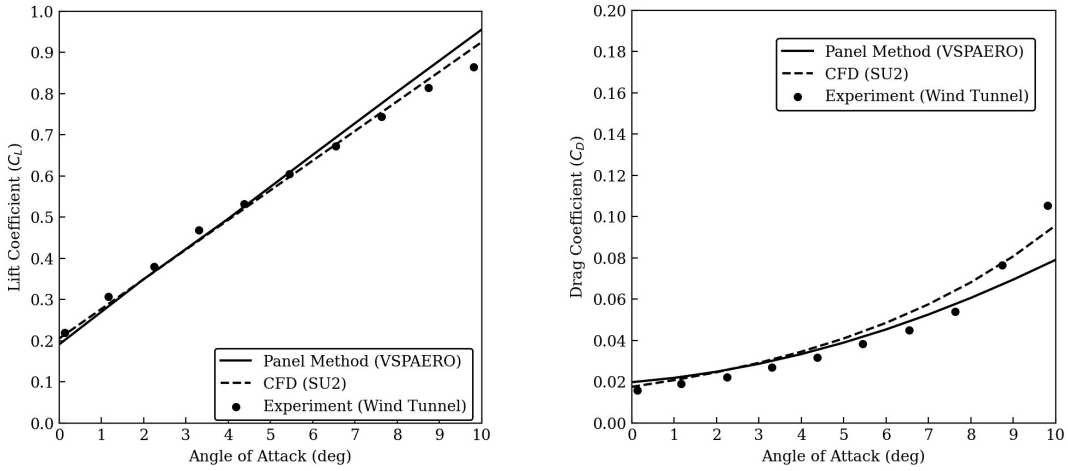

Fig. 7 Test Case: Comparison of lift and total drag coefficients

Further, the results of the high fidelity aerodynamic model are also evaluated in this graph. As expected, the CFD method is able to calculate the lift and drag coefficients more accurately. Results can be improved with changes in analysis settings, but this is beyond the focus of the paper.

IV. Surrogate Performance Modelling via Machine Learning

One of the key challenges in the design of UCAVs is the lack of fast and precise aerodynamic performance digital twins that can be utilized as a part of the optimization cycles. Toward this objective, in this study, we generate a black-box function that can predict the aerodynamic characteristics of UCAV configurations including compressibility effects by using deep learning algorithms. To be specific, an artificial neural network architecture is designed and trained using the data set created by the aerodynamic analysis models presented in the previous section. Thus, an instant solution can be provided using only geometry and flow parameters, without the need for analysis loops to calculate the performance of a new configuration.

A. Data Generation

In Table 3, geometry parameters and ranges for wing configurations are given. Each configuration was analyzed using high fidelity tool for two different Mach numbers: 0.5 and 0.6. The Latin hypercube sampling (LHS) was used for generating a quasi-random sampling distribution [62]. Thanks to this algorithm, it is possible to cover all design space with a limited data point.

Table 3 Geometry parameters and ranges

Surface	Airfoil	Root Chord	Span	Taper Ratio	Sweep	Mach
Wing	NACA 64-008A	3m	7m - 14m	0 - 1	0°- 40°	0.5 and 0.6

In this study, the initial data set with 1250 configurations (2500 total data points for two different Mach numbers) were used, but this number can be increased with various geometric combinations. Example wing configurations of the dataset generation algorithm are given in Fig. 8. As can be seen in the figure, configurations with different characteristic features have been produced in terms of various wingspans, taper ratios, and sweep angles.

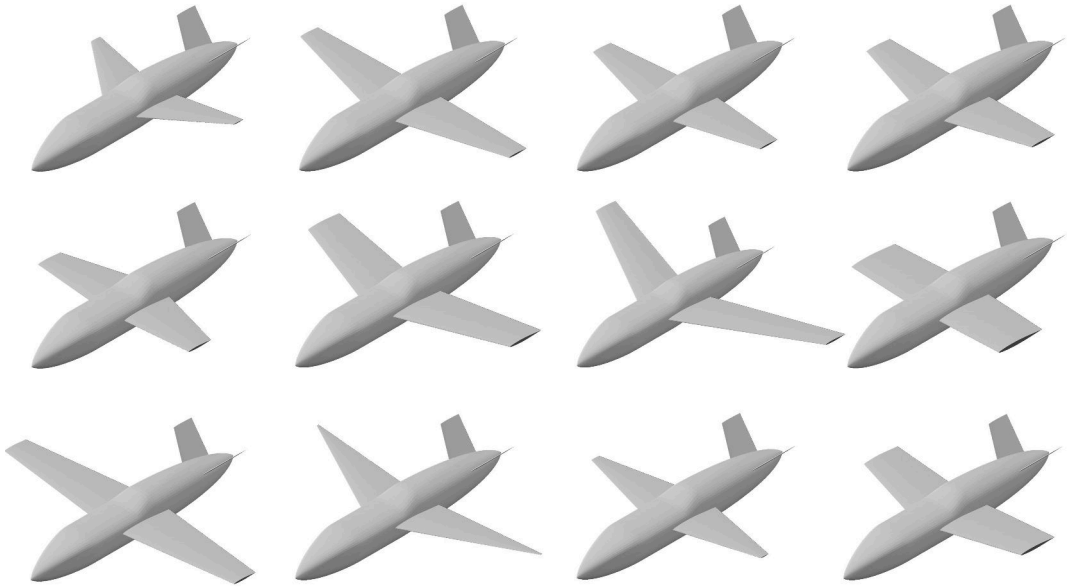

Fig. 8 Example wing configurations of the dataset generation algorithm

In addition, a total of 4500 data points were produced using the low fidelity tool to be used in the transfer learning algorithm. Some configurations in this dataset also have results at flow conditions between 0.5 and 0.6 Mach.

B. Feature Extraction

To determine feature parameters, the initial data set is examined. In order to evaluate the relationship between parameters, the correlation matrix was calculated with Pearson's method. In Fig. 9, positive correlations between parameters are shown in dark blue and negative correlations in light blue. The color densities are proportional to the correlation values.

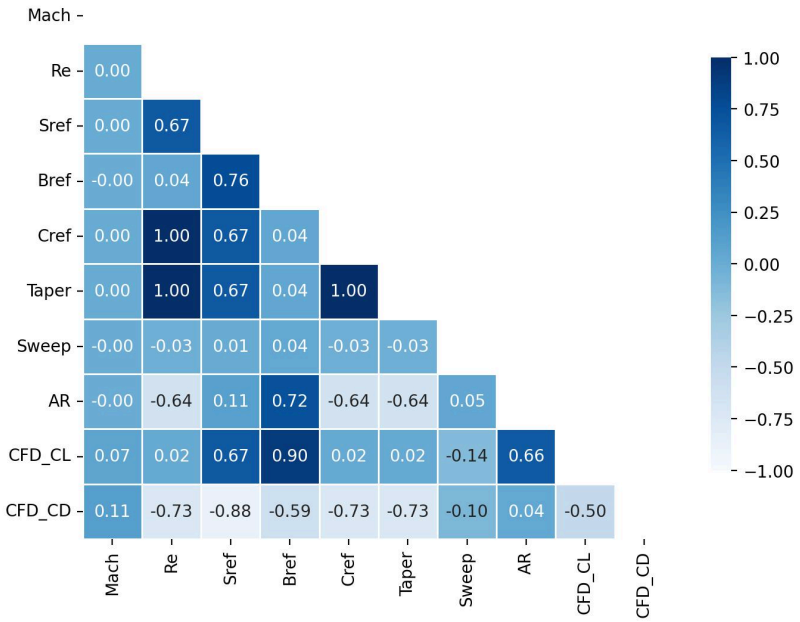

Fig. 9 Correlation matrix of the data set

Figure 10 illustrates how the lift coefficient data presents these correlations. As it can be seen from Mach number - lift coefficient figure, there is no high fidelity data at intermediate points in flow conditions. Input features for the models are extracted through aerodynamic equations and Pearson correlation analysis applied to the data.

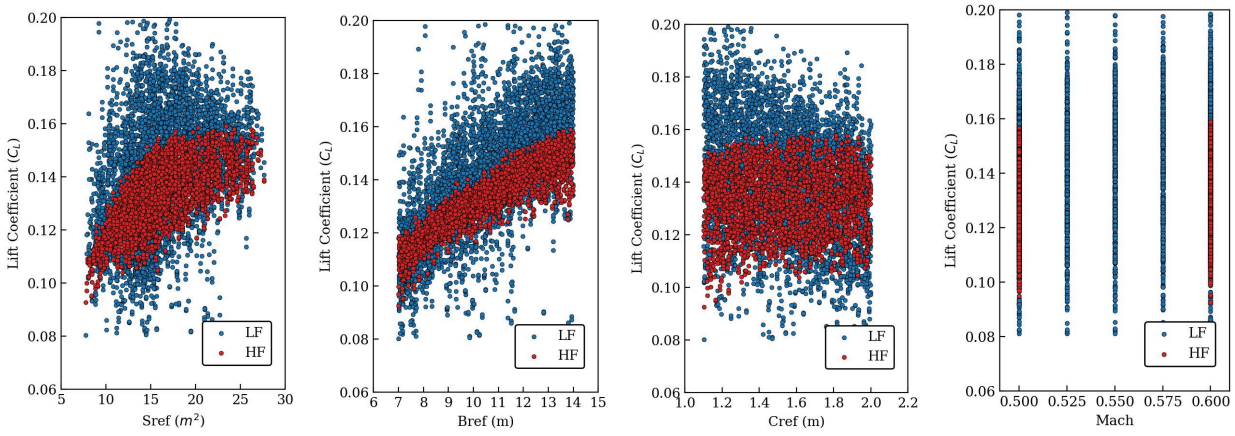

Fig. 10 Lift coefficient respect to feature parameters

Before training the model, the data set was examined to detect and to clear anomalies in the calculated performance parameters. At this point, it is very important to precisely stratify and shuffle the data set to ensure proper training and prevent undesired situations. In addition, the data set was divided into three groups: test, train, and validation. First, 95% of the data set was reserved for training and 5% for testing. In the next step, 10% of the training set was used for validation.

C. Artificial Neural Networks Model

In this subsection, the artificial neural network structure and its mathematical basis are explained in detail. As an initial model structure, the classical backpropagation algorithm performs learning on multilayer feed-forward neural network was used. Then, the Network-Based Deep Transfer Learning approach was used to train these models.

Before establishing the network structure, the training and the test sets are individually scaled to prevent the convergence problem caused by the difference in the magnitude of the inputs. As shown in Eq. 11, min-max scaling was applied to the dataset.

$$x_j^{sc} = \frac{x_j - \min(x)}{\max(x) - \min(x)} \tag{11}$$

A multi-layer perceptron architecture was built to predict the aerodynamic performance coefficients, Y, using X. For a fully-connected network with L hidden layers, this amounts to the following modeling equations relating the input features x, to its target prediction y.

A generic structure of a deep neural network consisting of a multilayer perceptron with M input features and N layers. It is composed of sequentially connected layers, which comprise sets of neurons that are combinations of mathematical operations followed by nonlinear activation functions. The model parameters ξ are defined as $\xi = \{W, b\}$, where $W = \{w_i\}_{i=1}^{N}$, and $b = \{b_i\}_{i=1}^{N}$. The output of the l_{th} layer is:

$$f(x, \xi_l) \quad = f_{w_l, b_l}(x) = z_l \left(\sum_{j=1}^{N_l} w_{lj} x_j + b_l \right) \tag{12}$$

$$= Z_l \left(w_l^T x_l + b_l \right) \quad (l = 1, \ldots, N) \tag{13}$$

where N_t is the neuron number and Z_l is a nonlinear activation function of a specific l_{th} layer, and x_l is the input of the l_{th} layer and also the output of the l-1_{th} layer. In addition to this, w_l and b_l are learnable parameters and called weight and bias terms of that layer respectively. Finally, the output of the last layer is a result of the composite and complex mapping defined as:

$$\hat{y}(x) := \left(f_{w_n, b_n} \circ \cdots \circ f_{w_1, b_1} \right)(x) \tag{14}$$

In transfer learning these learnable parameters, w_l and b_l , are shared between the models to extract knowledge from some related domains to help a neural network algorithm to achieve better performance. Finally, a neural network model is built to predict the lift coefficient by using the parameters summarized in Table 4.

Table 4 Hyperparameters for the artificial neural network architecture

Parameters	Values
Number of Hidden Layers	5
Neurons in the 1^{st}	256
Neurons in the 2^{nd}	128
Neurons in the 3^{rd}	64
Neurons in the 4^{th}	32
Neurons in the 5^{th}	16
Activation Function	ReLU
Optimizer	Adamax
Initializer	HE Normal
Loss Function	MAE
Batch Size	32
Epoch Number	500

Initially, a discrete model was trained with only high fidelity data for comparison purposes. In the next step, a new model was trained using the low-fidelity data. Then, some of the weight and bias parameters of this model was carried to the high-fidelity model training. The learning curves of the high-fidelity and transfler learning models are shown in Fig. 11, respectively.

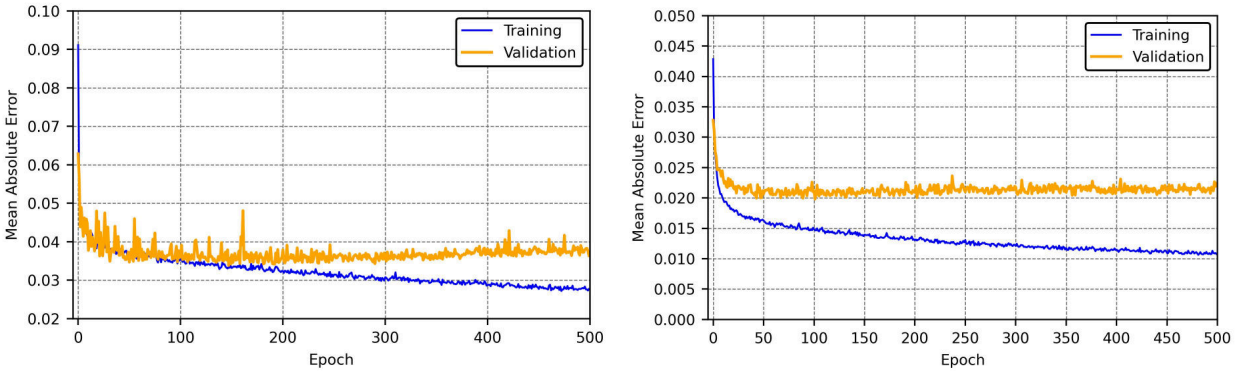

Fig. 11 Learning curves of high fidelity model and transfer learning model

V. Applications of the Model

In this section, the outcomes of several test examples of the current surrogate model are presented to show its prediction and generalization capability. For this purpose, the performance of different configurations in the test set tried to be estimated with the AI model.

The results reveal high-accuracy estimations with mean absolute errors of 0.0028 for the high fidelity model and 0.0027 for the transfer learning model. To monitor the success of the entire test set of the models, the value of the coefficient of determination, R^2, is calculated and the results are visualized in Fig. 12. In these figures, the x-axis and y-axis represent the real and predicted lift coefficient values, respectively. Each dot in the figure illustrates a different UCAV configuration. The value of R^2 was obtained in the order of 0.93 in both models. When the R^2 values are examined, it can be thought that there is no improvement in the prediction capacity of the model. However, the new model obtained by transfer learning increased the estimation capacity of the high fidelity model by using the information extracted from the low-fidelity model about the Mach number-lift coefficient relationship. It is possible to examine this situation specifically over the mach-lift coefficient curve of a generic configuration. As previously explained, the HF-model had only 0.5 and 0.6 Mach numbers data and was trained with this sparse data. In the LF-model, there were data from 0.5, 0.525, 0.55, 0.575 and 0.6 Mach numbers (see Fig. 10.

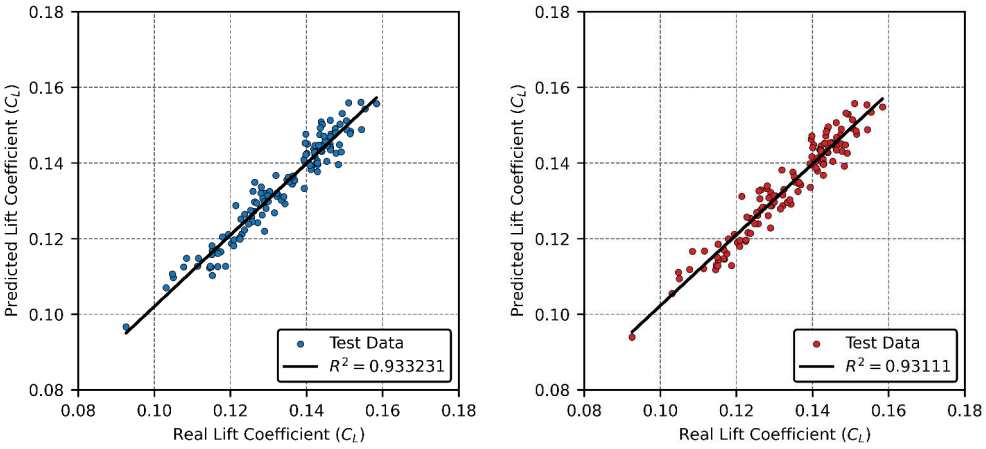

Fig. 12 High fidelity (HF) model (MAE: 0.0028) and transfer learning (TL) model (MAE: 0.0027) performances for target lift coefficient

However, the new model obtained by transfer learning increased the estimation capacity of the high fidelity model by using the information extracted from the low-fidelity model about the Mach number-lift coefficient relationship. It is possible to examine this situation specifically over the mach-lift coefficient curve of a generic configuration. As

previously explained, the HF-model had only 0.5 and 0.6 Mach number data and was trained with this sparse data. In the LF-model, there were data from 0.5, 0.525, 0.55, 0.575 and 0.6 Mach numbers (see Fig. 10.

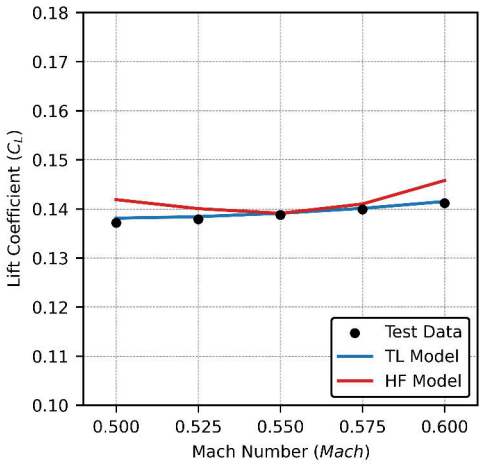

Fig. 13 Mach number - Lift coefficient curve for a generic configuration

As can be seen from Fig. 13, the prediction accuracy of the high fidelity (HF) model is not as successful as the transfer learning (TL) model. While the Mach number and the lift coefficient are expected to increase together, the high fidelity model could not catch this physical relationship due to the sparse dataset. However, thanks to Transfer learning, this effect has been properly modeled with the multifidelity approach.

In addition, an artificial neural networks model was developed for the drag coefficient prediction. In the Fig. 14, the x-axis and y-axis represent the real and predicted drag coefficient values, respectively. This time the value of R^2 was obtained in the order of 0.91 in high fidelity model. This level of accuracy is acceptable, especially of the conceptual and preliminary design phases. There was no need to develop a transfer learning algorithm for drag coefficient. However further implementations are possible to predict drag components.

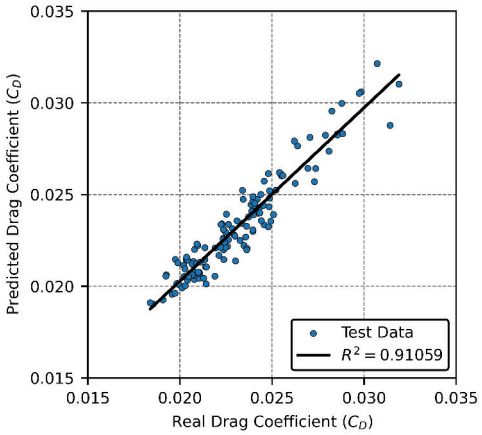

Fig. 14 High fidelity (HF) model (MAE: 0.00068) performance for target drag coefficient

The results obtained are generally satisfactory. However, this study was conducted on a very limited data set. As the success of deep learning algorithms increases as the dataset grows, it is possible to further improve the current results with larger training data.

VI. Conclusions

Major improvements in autonomy indicate that war environments will change rapidly in the future. In this concept, modular air vehicles, which stand out as a low-cost solution for different mission scenarios, also require cost-oriented practical approaches in design, production and certification. It is possible to solve these problems with fast and computationally inexpensive modeling tools. This paper presents a new machine learning based surrogate model to predict the aerodynamic performance of combat UAVs. Thanks to the developed model, it will possible to quickly analyze the main wing sets for different mission requirements. In addition, using the transfer learning approach, the performance of the model has been increased with the multifidelity approach in flow conditions where the database is sparse. The algorithm will capable of calculating the performance of a given geometry in milliseconds. This will be particularly interesting for digital twin and virtual certification processes.

Acknowledgments

Hasan Karali is co-funded by the EPSRC and the BAE Systems under 210085 numbered Industrial CASE award : *Towards Trustworthy AI-driven Autonomous Systems: Multi-Disciplinary Design Optimisation*.

References

[1] Humphreys, C., Cobb, R., Jacques, D., and Reeger, J., "Optimal mission path for the uninhabited loyal Wingman," *16th AIAA/ISSMO Multidisciplinary Analysis and Optimization Conference*, 2015, p. 2792.

[2] Stensrud, R., Mikkelsen, B., Betten, S., and Valaker, S., "A proposal for a simple evaluation method in support of the initial concept phase assessing a future unmanned Loyal Wingman for Royal Norwegian Air Force (RNoAF)," *38th International Symposium on Military Operational Research (38 ISMOR)*, 2021.

[3] Harper, J., "The Rise of Skyborg: Air Force Betting on New Robotic Wingman," *National Defense*, 2020. URL https://www.nationaldefensemagazine.org/articles/2020/9/25/air-force-betting-on-new-robotic-wingman.

[4] Gunzinger, M., and Autenried, L., "Understanding the Promise of Skyborg and Low-Cost Attritable Unmanned Aerial Vehicles," *Mitchell Institute Policy Paper*, Vol. 24, 2020.

[5] Reim, G., "Analysis: US Air Force eyes adoption of 'Loyal Wingman' UAVs," *Flight Global*, 2018. URL https://www.flightglobal.com/analysis/analysis-us-air-force-eyes-adoption-of-loyal-wingman-uavs/129330.article.

[6] Roblin, S., "F-35A Jet Price To Rise, But It's Sustainment Costs That Could Bleed Air Force Budget Dry," *Forbes Aerospace & Defense*, 2021. URL https://www.forbes.com/sites/sebastienroblin/2021/07/31/f-35a-jet-price-to-rise-but-its-sustainment-costs-that-could-bleed-air-force-budget-dry/?sh=6406d1b332df.

[7] Smith, A., and Rogers, M., 2021. URL https://www.gao.gov/products/gao-21-439.

[8] Colombi, J., Bentz, B., Recker, R., Lucas, B., and Freels, J., "Attritable design trades: Reliability and cost implications for unmanned aircraft," *2017 Annual IEEE International Systems Conference (SysCon)*, IEEE, 2017, pp. 1–8.

[9] Lt. Gen. Richard W. Scobee, "In Reserve, Question & Answers," *Air Force Magazine*, 2019, p. 36–37.

[10] Perrett, B., "Loyal wingmen could be the last aircraft standing in a future conflict," *The Strategist*, 2021. URL https://www.aspistrategist.org.au/loyal-wingmen-could-be-the-last-aircraft-standing-in-a-future-conflict/.

[11] AFRL, "SKYBORG: Open...Resilient...Autonomous," 2021. URL https://cdn.afresearchlab.com/wp-content/uploads/2020/02/03155042/AFRL_Skyborg_FS_0921.pdf.

[12] Pittaway, N., "Boeing details MQ-28A payload ground test phase," *Australian Defence Magazine*, 2022. URL https://www.australiandefence.com.au/defence/air/boeing-details-mq-28a-payload-ground-test-phase.

[13] Newdick, T., "The United Kingdom Has Chosen Who Will Build Its First Prototype Loyal Wingman Combat Drone," *The Drive The Warzone*, 2021. URL https://www.thedrive.com/the-war-zone/38898/the-united-kingdom-has-chosen-who-will-build-its-first-prototype-loyal-wingman-combat-drone.

[14] Boeing Defense, *Loyal Wingman*, Boeing Airpower Teaming System, ???? URL https://www.boeing.com/defense/airpower-teaming-system/#/gallery.

[15] Hoskins, S. A. J., *The XQ-58A Valkyrie pictured during a second test flight*, Wright-Patterson Air Force Base, 2019. URL https://www.wpafb.af.mil/News/Photos/igphoto/2002097026/.

[16] EADS, *Military Drone EADS Barracuda*, The European Aeronautic Defence and Space Company (EADS), ????

[17] Som, V., *An animated image of 2 unmanned Warrior drones flying in support of a Tejas Light Combat Aircraft*, NDTV, 2021. URL https://www.ndtv.com/india-news/exclusive-how-indias-new-warrior-drone-can-help-reshape-air-combat-2361475.

[18] Northrop Grumman, *Project Mosquito*, NG, ???? URL https://www.northropgrumman.com/what-we-do/air/project-mosquito/.

[19] GA Aeronautical Systems, *GA-ASI Introduces Gambit*, GA, ???? URL https://www.ga.com/ga-asi-introduces-gambit.

[20] "WBIs Problem Deconstruction Techniques Boost Digital Engineering in AFRL Vanguards," *Wright Brothers Institute*, 2020. URL https://www.wbi-innovates.com/blogs/post/VaDER.

[21] AIAA Digital Engineering Integration Committee, "Digital Twin: Definition & Value—An AIAA and AIA Position Paper," *AIAA: Reston, VA, USA*, 2020.

[22] "Boeing is accelerating the Joint Force's digital revolution," *Boeing*, 2021. URL https://www.boeing.com/defense/jadc2/digital-acceleration/index.page.

[23] Cummings, R. M., Mason, W. H., Morton, S. A., and McDaniel, D. R., *Applied Computational Aerodynamics: A Modern Engineering Approach*, Cambridge Aerospace Series, Cambridge University Press, 2015. https://doi.org/10.1017/CBO9781107284166.

[24] Li, J., Du, X., and Martins, J. R., "Machine Learning in Aerodynamic Shape Optimization," *arXiv preprint arXiv:2202.07141*, 2022.

[25] Ahn, J., Kim, H.-J., Lee, D.-H., and Rho, O.-H., "Response surface method for airfoil design in transonic flow," *Journal of aircraft*, Vol. 38, No. 2, 2001, pp. 231–238.

[26] Andrés-Pérez, E., Carro-Calvo, L., Salcedo-Sanz, S., and Martin-Burgos, M. J., "Aerodynamic shape design by evolutionary optimization and support vector machines," *Application of Surrogate-based Global Optimization to Aerodynamic Design*, Springer, 2016, pp. 1–24.

[27] Han, Z., Zhang, K., Song, W., and Liu, J., "Surrogate-based aerodynamic shape optimization with application to wind turbine airfoils," *51st AIAA aerospace sciences meeting including the new horizons forum and aerospace exposition*, 2013, p. 1108.

[28] Xu, J., Han, Z., Yan, X., and Song, W., "Aerodynamic Design of Megawatt Wind Turbine Blades with NPU-WA Airfoils," *IOP Conference Series: Earth and Environmental Science*, Vol. 495, IOP Publishing, 2020, p. 012018.

[29] Li, J., Bouhlel, M. A., and Martins, J. R., "Data-based approach for fast airfoil analysis and optimization," *AIAA Journal*, Vol. 57, No. 2, 2019, pp. 581–596.

[30] Du, X., and Leifsson, L., "Optimum aerodynamic shape design under uncertainty by utility theory and metamodeling," *Aerospace Science and Technology*, Vol. 95, 2019, p. 105464.

[31] Lin, Q., Chen, C., Xiong, F., Chen, S., and Wang, F., "An improved PC-Kriging method for efficient robust design optimization," *International Conference on Mechanical Design*, Springer, 2019, pp. 394–411.

[32] Nagawkar, J., and Leifsson, L., "Applications of Polynomial Chaos-Based Cokriging to Simulation-Based Analysis and Design Under Uncertainty," *International Design Engineering Technical Conferences and Computers and Information in Engineering Conference*, Vol. 84010, American Society of Mechanical Engineers, 2020, p. V11BT11A046.

[33] Bouhlel, M. A., He, S., and Martins, J. R., "Scalable gradient–enhanced artificial neural networks for airfoil shape design in the subsonic and transonic regimes," *Structural and Multidisciplinary Optimization*, Vol. 61, No. 4, 2020, pp. 1363–1376.

[34] Du, X., He, P., and Martins, J. R., "A B-spline-based generative adversarial network model for fast interactive airfoil aerodynamic optimization," *AIAA Scitech 2020 Forum*, 2020, p. 2128.

[35] Barnhart, S. A., Narayanan, B., and Gunasekaran, S., "Blown wing aerodynamic coefficient predictions using traditional machine learning and data science approaches," *AIAA Scitech 2021 Forum*, 2021, p. 0616.

[36] Yu, B., Xie, L., and Wang, F., "An improved deep convolutional neural network to predict airfoil lift coefficient," *International Conference on Aerospace System Science and Engineering*, Springer, 2019, pp. 275–286.

[37] Zhang, Y., Sung, W. J., and Mavris, D. N., "Application of convolutional neural network to predict airfoil lift coefficient," *2018 AIAA/ASCE/AHS/ASC structures, structural dynamics, and materials conference*, 2018, p. 1903.

[38] Zhang, X., Xie, F., Ji, T., Zhu, Z., and Zheng, Y., "Multi-fidelity deep neural network surrogate model for aerodynamic shape optimization," *Computer Methods in Applied Mechanics and Engineering*, Vol. 373, 2021, p. 113485.

[39] Sohst, M., Vale, J., Crawford, C., Potter, G., and Banerjee, S., "A framework for multi-fidelity multi-disciplinary kriging-based surrogate model optimization of novel aircraft configurations," *NATO STO-MP-AVT-324*, ????

[40] Jesus, T., Sohst, M., Vale, J. L. d., and Suleman, A., "Surrogate based MDO of a canard configuration aircraft," *Structural and Multidisciplinary Optimization*, Vol. 64, No. 6, 2021, pp. 3747–3771.

[41] Setayandeh, M. R., "Surrogate Model–Based Robust Multidisciplinary Design Optimization of an Unmanned Aerial Vehicle," *Journal of Aerospace Engineering*, Vol. 34, No. 4, 2021, p. 04021029.

[42] Yang, S., and Yee, K., "Design rule extraction using multi-fidelity surrogate model for unmanned combat aerial vehicles," *Journal of Aircraft*, 2022, pp. 1–15.

[43] Shi, Q., Wang, H., Cheng, H., Cheng, F., and Wang, M., "An Adaptive Sequential Sampling Strategy-Based Multi-Objective Optimization of Aerodynamic Configuration for a Tandem-Wing UAV via a Surrogate Model," *IEEE Access*, Vol. 9, 2021, pp. 164131–164147.

[44] Andrés-Pérez, E., and Paulete-Periáñez, C., "On the application of surrogate regression models for aerodynamic coefficient prediction," *Complex & Intelligent Systems*, Vol. 7, No. 4, 2021, pp. 1991–2021.

[45] Keane, A. J., and Voutchkov, I. I., "Surrogate approaches for aerodynamic section performance modeling," *AIAA Journal*, Vol. 58, No. 1, 2020, pp. 16–24.

[46] Karali, H., Demirezen, M. U., Yukselen, M. A., and Inalhan, G., "Design of a Deep Learning Based Nonlinear Aerodynamic Surrogate Model for UAVs," *AIAA Scitech 2020 Forum*, Orlando, FL, 2020, p. 1288. https://doi.org/10.2514/6.2020-1288.

[47] Karali, H., Yukselen, M. A., and Inalhan, G., "A New Non-Linear Lifting Line Method for 3D Analysis of Wing/Configuration Aerodynamic Characteristics with Application to UAVs," *AIAA Scitech 2019 Forum*, San Diego, CA, 2019, p. 2119. https://doi.org/10.2514/6.2019-2119.

[48] Karali, H., Inalhan, G., Umut Demirezen, M., and Adil Yukselen, M., "A new nonlinear lifting line method for aerodynamic analysis and deep learning modeling of small unmanned aerial vehicles," *International Journal of Micro Air Vehicles*, Vol. 13, 2021, p. 17568293211016817.

[49] Pan, S. J., and Yang, Q., "A survey on transfer learning," *IEEE Transactions on knowledge and data engineering*, Vol. 22, No. 10, 2009, pp. 1345–1359.

[50] Pan, S. J., "Transfer learning," *Learning*, Vol. 21, 2020, pp. 1–2.

[51] Tan, C., Sun, F., Kong, T., Zhang, W., Yang, C., and Liu, C., "A survey on deep transfer learning," *International conference on artificial neural networks*, Springer, 2018, pp. 270–279.

[52] Weiss, K., Khoshgoftaar, T. M., and Wang, D., "A survey of transfer learning," *Journal of Big data*, Vol. 3, No. 1, 2016, pp. 1–40.

[53] Economon, T. D., Palacios, F., Copeland, S. R., Lukaczyk, T. W., and Alonso, J. J., "SU2: An open-source suite for multiphysics simulation and design," *Aiaa Journal*, Vol. 54, No. 3, 2016, pp. 828–846.

[54] Kinney, D., and McDonald, R., "VSPAero/OpenVSP Integration," , 2015.

[55] Garcia, J. A., Bowles, J. V., Kinney, D. J., Melton, J. E., and Jiang, X. J., "VIPER Integrated MDAO Analysis for Conceptual Design of Supersonic X-Plane Vehicles," Tech. rep., 2019.

[56] McDonald, R. A., "Advanced modeling in OpenVSP," *16th AIAA Aviation Technology, Integration, and Operations Conference*, 2016, p. 3282.

[57] McDonald, R. A., and Gloudemans, J. R., "Open Vehicle Sketch Pad: An Open Source Parametric Geometry and Analysis Tool for Conceptual Aircraft Design," *AIAA SCITECH 2022 Forum*, 2022, p. 0004.

[58] Geuzaine, C., and Remacle, J.-F., "Gmsh: A 3-D finite element mesh generator with built-in pre-and post-processing facilities," *International journal for numerical methods in engineering*, Vol. 79, No. 11, 2009, pp. 1309–1331.

[59] Erickson, L. L., "Panel methods: An introduction," Tech. rep., 1990.

[60] Katz, J., and Plotkin, A., *Low-speed aerodynamics*, Vol. 13, Cambridge university press, 2001.

[61] "Compressible Euler," *Governing Equations in SU2*, ???? URL https://su2code.github.io/docs_v7/Theory/#compressible-euler.

[62] Bouhlel, M. A., Hwang, J. T., Bartoli, N., Lafage, R., Morlier, J., and Martins, J. R. R. A., "A Python surrogate modeling framework with derivatives," *Advances in Engineering Software*, 2019, p. 102662. https://doi.org/https://doi.org/10.1016/j.advengsoft.2019.03.005.

2023-01-19

AI-based multifidelity surrogate models to develop next generation modular UCAVs

Karali, Hasan

AIAA

Karali H, Inalhan G, Tsourdos A. (2023) AI-based multifidelity surrogate models to develop next generation modular UCAVs. In: AIAA SciTech Forum 2023, 23-27 January 2023, National Harbor, Maryland, USA. Paper number AIAA 2023-0670

https://doi.org/10.2514/6.2023-0670